Metallophysics and Advanced Technologies
Металофіз. новітні технол.
Metallofiz. Noveishie Tekhnol.
2025, vol. 47, No. 6, pp. 581–594
https://doi.org/10.15407/mfint.47.06.0581
Reprints available directly from the publisher

PACS numbers: 71.70.Ej, 75.30.Ds, 75.30.Et, 75.50.Ee, 75.70.Tj, 75.85.+t, 85.70.Ay

Electric-Field Control of the Temporal Attenuation of Right-Handed and Left-Handed Magnons in Antiferromagnets

O. O. Boliasova[*,**] and V. M. Krivoruchko[***]

[*]*G. V. Kurdyumov Institute for Metal Physics, N.A.S. of Ukraine,*
36 Academician Vernadsky Blvd.,
UA-03142 Kyiv, Ukraine
[**]*Kyiv Academic University, N.A.S. and M.E.S. of Ukraine,*
36 Academician Vernadsky Blvd.,
UA-03142 Kyiv, Ukraine
[***]*Donetsk Institute for Physics and Engineering Named after O. O. Galkin,*
N.A.S. of Ukraine,
46 Nauky Ave.,
03028 Kyiv, Ukraine

Spin waves in antiferromagnets are promising alternative for replacing semiconductor technologies in future computational devices. One of the unique features of antiferromagnets is the availability of two spin waves with different chiralities—right-handed and left-handed ones. This degree of freedom, in addition to their phase and amplitude, can be used to create modern computational devices. The search for an effective method to separate and control the two modes in antiferromagnets is now attracting the increasing attention. Previous studies have demonstrated that an electric field can manipulate antiferromagnetic magnons of different chiralities. However, the influence of the Aharonov–Casher effect on the damping right-handed and left-handed spin waves has not been fully investigated. In this work, based on Landau–Lifshitz–Gilbert equations with Rayleigh-dissipation functional, we show that the applied electric field could effectively control the damping of the spin waves with different chiralities. Temporal attenuation of the right-

Corresponding author: Ol'ha Oleksandrivna Boliasova
E-mail: ol.boliasova@gmail.com

Citation: O. O. Boliasova and V. M. Krivoruchko, Electric-Field Control of the Temporal Attenuation of Right-Handed and Left-Handed Magnons in Antiferromagnets, *Metallofiz. Noveishie Tekhnol.*, **47**, No. 6: 581–594 (2025). DOI: 10.15407/mfint.47.06.0581

handed and left-handed modes has a shift along the wave-vector axis, which is directly proportional to the magnitude of the electric field. The relation between the damping parameters in the Rayleigh-dissipation functional plays an important role in dissipation behaviour. Our results show that the magnon lifetime depends on the electric field and dissipation parameters and is different for distinct chiralities. We believe our findings will encourage further investigation into dissipation processes in antiferromagnets and their impact on magnonic devices.

Key words: spin-wave dynamics, antiferromagnets, Aharonov–Casher effect, damping, Gilbert damping, right-handed and left-handed polarizations, Landau–Lifshitz–Gilbert equation.

Спінові хвилі в антиферомагнетиках розглядаються як перспективна альтернатива напівпровідниковим технологіям в майбутніх обчислювальних пристроях. Однією з ключових особливостей антиферомагнетиків є наявність двох спінових мод з різними хіральностями — правосторонньою та лівосторонньою. Цей додатковий ступінь свободи, разом із фазою й амплітудою, може бути використаний для створення новітніх магнонних обчислювальних систем. Пошук ефективних методів розщеплення та керування зазначеними модами в антиферомагнетиках наразі є предметом активних досліджень. Дослідження показують, що за допомогою електричного поля можна керувати антиферомагнетними магнонами з різною хіральністю. Водночас вплив ефекту Ааронова–Кашера на згасання спінових хвиль з правою та лівою поляризаціями залишається недостатньо вивченим. У даній роботі на основі рівнянь Ландау–Ліфшиця–Гілберта з урахуванням функціоналу Релейової дисипації продемонстровано, що прикладене електричне поле здатне ефективно контролювати згасання спінових хвиль з різною хіральністю. Показано, що часове згасання правосторонніх і лівосторонніх мод супроводжується зсувом уздовж осі хвильового вектора, який є прямо пропорційним до величини електричного поля. Встановлено, що співвідношення між параметрами функціоналу Релейової дисипації відіграє визначальну роль у дисипації. Результати роботи свідчать, що час життя магнонів залежить від електричного поля, параметрів дисипації та відрізняється для різних хіральностей. Одержані висновки відкривають перспективи для подальшого вивчення механізмів дисипації в антиферомагнетиках і їхнього впливу на магноніку.

Ключові слова: динаміка спінових хвиль, антиферомагнетики, ефект Ааронова–Кашера, дисипація, Гілбертова дисипативна константа, правостороння та лівостороння поляризації, рівняння Ландау–Ліфшиця–Гілберта.

(Received 2 June, 2025; in final version, 16 June, 2025)

1. INTRODUCTION

Magnonics [1], a recent branch of condensed matter physics, has

gained significant interest due to its potential to use spin waves (SWs) as carriers of information in electronic devices [2]. Spin waves can propagate without Joule heating and allow high operational speeds. Antiferromagnets (AFMs), due to the antiparallel arrangement of the two magnetic sublattices, can simultaneously support left-handed and right-handed polarized spin waves (SWs), providing an extra degree of freedom—chirality. Due to their stability to small field perturbations and absence of the stray field, AFMs are promising candidates for developing devices that incorporate spin waves.

Currently, there are several methods for manipulating SWs, for example, magnetic field, a Dzyaloshinskii–Moriya interaction in curvilinear magnets, spin-transfer torque, spin–orbit torque, spin Seebeck effect, voltage-controlled magnetic anisotropy, optical methods, and electric field. We will focus on the electric (**E**) field effect based on the so-called Aharonov–Casher (AC) effect [3, 4]. The AC effect, a quantum mechanical phenomenon like the Aharonov–Bohm effect, appears when a neutral particle with a magnetic moment moves under the effect of an **E** field and acquires a phase shift in the particle's wave function. In work [5], Cao and co-authors have demonstrated that the AC effect influences SWs propagating in a ferromagnetic ring when an **E** field is applied. Recent theoretical [6, 7] and experimental [8, 9] studies have demonstrated that the AC effect could impact SW propagation by using a static electric field in various magnetic systems, including AFMs, providing a mechanism for electric-field-based control of magnon dynamics.

It has been shown that in the first approximation, the influence of the AC effect on SWs can be mathematically represented as a Dzyaloshinskii–Moriya (DM)-like interaction [10, 11]. DM interaction, a form of antisymmetric exchange coupling, plays a crucial role in chiral magnetic systems with breaking inversional symmetry, resulting in SW nonreciprocity. In this context, the AC effect could effectively modify the spin-waves' dispersion relation in a symmetric crystal, lifting the energy degeneracy of two magnon modes by the applied electric field. As a result, SWs in antiferromagnetic materials can be distinctly separated into right-handed and left-handed modes [7].

One of the methods to split SWs in an AFM with different chirality is to induce the DM interaction, for example, by bending a material and breaking its symmetry. One of the disadvantages of this method is that one should bend it again to change the spin wave spectrum. At the same time, using the AC effect allows one to change the spin-waves' spectrum by applying an electric field, which is easier to incorporate in real devices. The unique advantages of this method include the strength and sign of the **E** field, which can be controlled, and the switchable nonreciprocity, which provides a potential platform for the design of magnonic devices.

Despite all advances in magnonic research, one critical aspect of SW dynamics remains unexplored. It is the influence of the AC effect on SWs energy dissipation. This article is dedicated to this question. Understanding how damping is affected by the topological AC effect is essential for a comprehensive description of magnons' dynamics and practical applications in antiferromagnetic-based magnonic devices [1, 12].

The dynamic characteristics of a dissipative (or absorbing) medium with finite damping include both real and imaginary components and are thus complex. There are two possible representations of the frequency and wave vector to describe the complex dispersion relation. One is the real frequency ω and the complex wave vector $\mathbf{k} = \mathrm{Re}\mathbf{k} + i\mathrm{Im}\mathbf{k}$; the other is the complex frequency $\omega = \mathrm{Re}\omega + i\mathrm{Im}\omega$ and the real wave vector $\mathbf{k}$, which is used widely in magnetism and spintronics communities. One can choose one of the two representations depending on the problem under investigation. The real ω and complex $\mathbf{k}$ focus on how the wave vector is affected by damping, and it is adequate to investigate the damping effect on propagating waves (see, for example, [13]). The complex ω and real $\mathbf{k}$ focus on how the frequency is affected by damping and describe the damping effect on the resonance, including the uniform magnetization dynamics. In this report, we use the last combination to demonstrate how the applied electric field modifies the SWs energy and damping in the two-sublattice AFM insulator. To derive analytical solutions, we used the set of the Landau–Lifshitz–Gilbert equations. There are two common options for how to adjust for damping: (i) including only the intrasublattice component [14], or (ii) a combination of intrasublattice and intersublattice components [15–17]. We will show how each of these options could modify the temporal damping, a so-called SW-regime [18], *i.e.*, spectrum width.

The paper is structured as follows: in the next Section, we will provide a brief explanation of the model used. In Section 3, our main results are presented. Section 4 is dedicated to discussing the results and presenting the conclusions derived from the study. Finally, we express our gratitude in acknowledgments.

2. THEORETICAL DETAILS

We consider the easy axis AFM consisting of two equivalent sublattices with magnetization $\mathbf{M}_1$ and $\mathbf{M}_2$. Further, for convenience, we will use unit vectors $\mathbf{m}_i = \mathbf{M}_i / M_s$, where i is the sublattice number ($i = 1, 2$), $\mathbf{M}_S \parallel Oz$ is sublattice saturation magnetization. Figure 1 shows the system view, where the electric field $\mathbf{E}$ is applied along the y-axis and magnons propagate along the x-axis.

Assuming the sublattices are equal and an AFM is symmetric under sublattice permutations, the free energy $F(\mathbf{m})$ of the system under con-

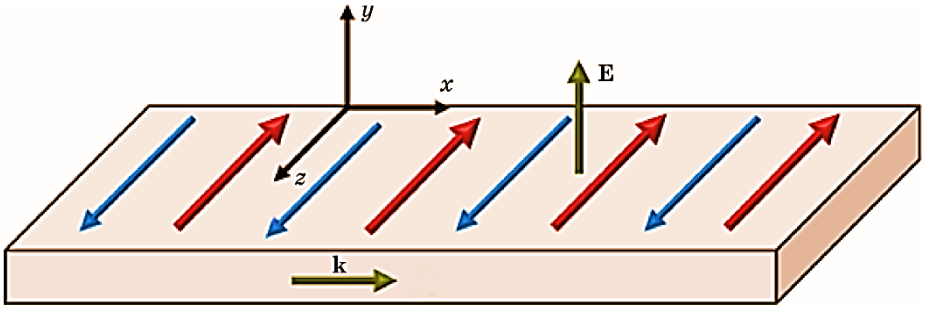

Fig. 1. Schematic representation of the antiferromagnet under electric field effect. Thin blue arrows along z direction and thick red arrows along $-z$ direction indicate the magnetization of the first and second sublattices accordingly. Electric field $\mathbf{E} \parallel Oy$, wave vector $\mathbf{k} \parallel Ox$.

sideration is:

$$F(\mathbf{m}) = \frac{A}{2}\int_V \left(\left(\frac{\partial \mathbf{m}_1}{\partial x}\right)^2 + \left(\frac{\partial \mathbf{m}_2}{\partial x}\right)^2 \right) dx + J\int_V (\mathbf{m}_1\mathbf{m}_2)dx - \\ -\frac{K}{2}\int_V \left(\mathbf{m}_1^2 + \mathbf{m}_2^2\right)dx + \frac{\mathbf{D}}{2}\int_V \left(\mathbf{m}_1 \times \frac{\partial \mathbf{m}_2}{\partial x} + \mathbf{m}_2 \times \frac{\partial \mathbf{m}_1}{\partial x} \right) dx. \quad (1)$$

The first two terms describe nonhomogeneous intrasublattices exchange coupling with a constant A, and homogeneous intersublattices' exchange coupling with a constant J. The next term corresponds to magnetocrystalline anisotropy with the anisotropy constant K. Here, the anisotropy along the z-axis is considered. The last term describes the effect of the electric field. In the first approximation, the AC effect mathematically could be incorporated in the form of the DM-like interaction $\mathbf{D}(\mathbf{m}_1 \times \mathbf{m}_2)$ [10, 11], where $\mathbf{D}$ is the vector depending on the applied electric field [6]:

$$\mathbf{D} = J\frac{ea}{E_{SO}}\mathbf{E} \times \mathbf{e}_{12} \equiv d\mathbf{E} \times \mathbf{e}_{12}. \quad (2)$$

Here, a is the distance between magnetic ions, e is the charge of the electron, $\mathbf{e}_{12}$ is unit vector in the direction connecting the ions from different sublattices, E_{SO} is energy of the spin–orbit interaction that inversely depends on the strength of the spin–orbit coupling. Recent studies [6] have shown that in some materials, E_{SO} could be around 1–3 eV, which makes this interaction valuable. As follows from Eq. (2), to achieve the maximum contribution from this interaction, the wave vector $\mathbf{k}$, the magnetization $\mathbf{m}_i$, and the electric field $\mathbf{E}$ should be orthogonal as in Fig. 1.

A phenomenological approach utilizes the Landau–Lifshitz–Gilbert

equation to describe the dynamics of magnetic materials. The equation with the dissipation term **R** is given by:

$$\frac{\partial \mathbf{m}}{\partial t} = -\gamma \mathbf{m} \times \mathbf{H}^{\text{eff}} + \mathbf{R},$$

where $\mathbf{H}^{\text{eff}} = -dF/d\mathbf{m}_i$ is the effective field, $\gamma = g\mu_0\mu_B / \hbar$ is the gyromagnetic ratio (here, g is the g factor, μ_0 is the magnetic permeability of the vacuum, μ_B is the Bohr magneton, $\hbar$ is the reduced Planck constant). In ferromagnets, the Gilbert dissipation term looks like $\mathbf{R} = \alpha_G \mathbf{m} \times \partial \mathbf{m}/\partial t$. When considering two-sublattice magnets, a question arises about how to account for the dissipation term. Some recent works [15, 16] argue for using the Rayleigh-dissipation functional as a matrix 2×2 with different damping coefficients. Thus, the two-sublattice magnet is described by the system of two torque equations with intrasublattice (α_{11}, α_{22}) and intersublattice (α_{12}, α_{21}) damping coefficients, which looks like:

$$\begin{aligned}
\frac{\partial \mathbf{m}_1}{\partial t} &= -\gamma \mathbf{m}_1 \times \mathbf{H}_1^{\text{eff}} + \alpha_{11}\mathbf{m}_1 \times \frac{\partial \mathbf{m}_1}{\partial t} + \alpha_{12}\mathbf{m}_1 \times \frac{\partial \mathbf{m}_2}{\partial t}, \\
\frac{\partial \mathbf{m}_2}{\partial t} &= -\gamma \mathbf{m}_2 \times \mathbf{H}_2^{\text{eff}} + \alpha_{21}\mathbf{m}_2 \times \frac{\partial \mathbf{m}_1}{\partial t} + \alpha_{22}\mathbf{m}_2 \times \frac{\partial \mathbf{m}_2}{\partial t}.
\end{aligned} \tag{3}$$

In AFM with equivalent sublattices, the number of damping parameters reduces to intrasublattice ($\alpha = \alpha_{11} = \alpha_{22}$) and intersublattice ($\alpha_c = \alpha_{12} = \alpha_{21}$) ones. It should be noted here that the damping within a sublattice should be greater than the damping between sublattices. In AFM, researchers commonly use one damping inside each sublattice α [14, 19]. Neglecting α_c implies that variables $\mathbf{m}_1$ and $\mathbf{m}_2$ are not directly connected in the damping processes. However, the magnetization of the two sublattices is coupled and cannot be missed during the discovery of the magnetization dynamics [17]. As is shown in the next Section, the **E** field also affects SWs' intersublattice attenuation.

3. AHARONOV–CASHER EFFECT ON TEMPORAL ATTENUATION OF SPIN WAVES

We assume that the AFM is in the collinear state and consider SWs with the frequency ω and wave $\mathbf{k}$ propagating along the x-axis, $\mathbf{k} \parallel Ox$, such that

$$\begin{aligned}
\mathbf{m}_1 &= \mathbf{x} m_{1x} \exp(i(\omega t - kx)) + \mathbf{y} m_{1y} \exp(i(\omega t - kx)) + \mathbf{z} m_{1z}, \\
\mathbf{m}_2 &= \mathbf{x} m_{2x} \exp(i(\omega t - kx)) + \mathbf{y} m_{2y} \exp(i(\omega t - kx)) + \mathbf{z} m_{2z},
\end{aligned}$$

with a small deviation of the magnetization of the first and second sub-

lattices along the z-axis $|m_{1z}| = |m_{2z}| \approx 1$. After obtaining the effective field from expression (1) and substituting it into the system of equations (3), we switch to circular variables defined as $m_{i+} = m_{ix} + im_{iy}$, $m_{i-} = m_{ix} - im_{iy}$. This allows us to derive a matrix consisting of two equations:

$$\begin{pmatrix} \pm\dfrac{M_S}{\gamma}\omega - P - i\alpha\omega & -W_{\pm} - i\alpha_c\dfrac{M_S}{\gamma}\omega \\ W_{\pm} + i\alpha_c\dfrac{M_S}{\gamma}\omega & \pm\dfrac{M_S}{\gamma}\omega + P + i\alpha\dfrac{M_S}{\gamma}\omega \end{pmatrix} \begin{pmatrix} m_{1\pm} \\ m_{2\pm} \end{pmatrix} = 0\,. \tag{4}$$

Here, we introduce the next notation $P = J + K + Ak^2$, $W_+ = J \pm kdE$. The determinant of this matrix describes the SW dynamics of the AFM. By setting the real and imaginary parts to zero, we can find the spin waves' energy $\omega_i(k)$ and damping $\Gamma_i(k)$, using the substitution $\omega = \omega(k) + i\Gamma(k)$. We will provide the analytical expressions for these values below.

3.1. Spin-Wave Spectrum

It was shown earlier [7, 13] that the applied electric field splits the SWs spectrum into right-handed and left-handed magnons. Here, we demonstrate the AC effect on the SW dynamics in our system. We start by setting to zero the real part of the determinant of matrix (4), which gives us the next expression:

$$\omega_{\pm}(k) = \frac{\gamma}{M_S}\sqrt{(Ak^2 \pm kdE + 2J + K)(Ak^2 \mp kdE + K)}\,. \tag{5}$$

The difference between the magnon frequency with right-handed polarization, ω_+, and left-handed polarization, ω_-, is in the sign of the electric field term: kdE. The SW spectrum in the absence and the presence of an applied electric field is depicted in Fig. 2. The shift along the wave vector axis is directly proportional to the magnitude of the applied electric field. The greater the applied **E** field, the larger the splitting between right- and left-handed polarization magnons' energy. For visualization, here and below, the following quantities were used $M_S = 3.5 \cdot 10^5$ A/m, $A = 2 \cdot 10^{-12}$ J/m, $J = 5 \cdot 10^6$ J/m^3, $K = 10^5$ J/m^3, lattice constant $a = 0.5$ nm, and parameter of our system $d = 4.4 \cdot 10^{-12}$ C/m. We should point out that reversing the direction of the applied electric field results in a swap between left- and right-handed SWs shift along the wave vector **k**.

3.2. Spin-Wave Damping

The interplay between magnons' spin polarization and magnetic damp-

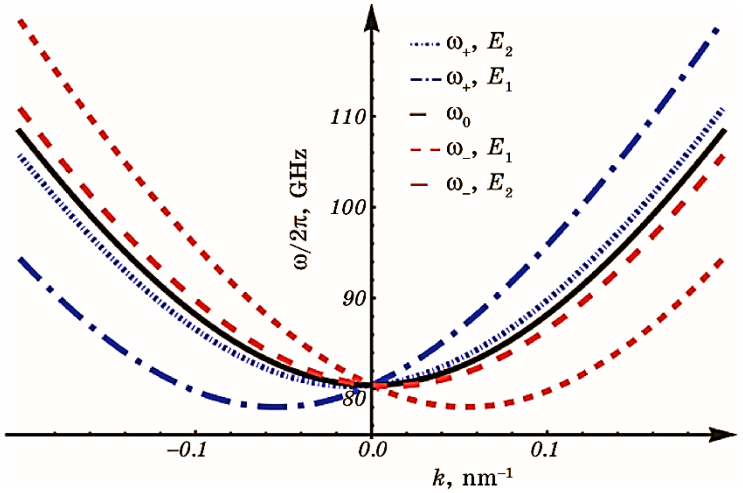

Fig. 2. Splitting of the spin wave spectrum under the **E** field effect, Eq. (5): $E_1 = 50$ V/μm, $E_2 = 10$ V/μm. The black line corresponds to $\mathbf{E} = \mathbf{0}$.

ing plays a crucial role in magnonics. We consider temporal decay, which could be found in resonance experiments as the width of the resonance peak [20]. This effect of AC has not been considered earlier.

Substituting $\omega = \omega(k) + i\Gamma(k)$ into matrix (4), we can get from the imaginary part of the determinant the following expression for temporal damping:

$$\Gamma_{\pm}(k) = \gamma \frac{\alpha(J + K + Ak^2) - \alpha_c(J \pm kdE)}{M_S(1 + \alpha^2 - \alpha_c^2)}. \tag{6}$$

As we see in Eq. (6), the external electric field affects SWs' damping through intersublattice damping coupling. The **E**-field application leads to the appearance of two attenuation functions $\Gamma_+(k)$ and $\Gamma_-(k)$. Like the frequency characteristics, the shift of the two attenuation curves depends on the value of the electric field (Fig. 3). Figure 4 shows temporal attenuation $\Gamma_{\pm}(k)$ at different values of the corresponding frequency $\omega_{\pm}(k)$.

We also found the ratio between the width of the resonance and its frequency $\Gamma_{\pm}(k)/\omega_{\pm}(k)$:

$$\frac{\Gamma_{\pm}(k)}{\omega_{\pm}(k)} = \frac{\alpha(J + K + Ak^2) - \alpha_c(J \pm kdE)}{(1 + \alpha^2 - \alpha_c^2)\sqrt{(J + K + Ak^2)^2 - (J \pm kdE)^2}}. \tag{7}$$

Figure 5 shows $\Gamma_{\pm}(k)/\omega_{\pm}(k)$ at different damping constants: $\alpha = 0.005$, $\alpha_c = 0.001$; $\alpha = 0.005$, $\alpha_c = 0.004$. As α_c has antidamping behaviour, the bigger this parameter is, the lower the ratio $\Gamma_{\pm}(k)/\omega_{\pm}(k)$.

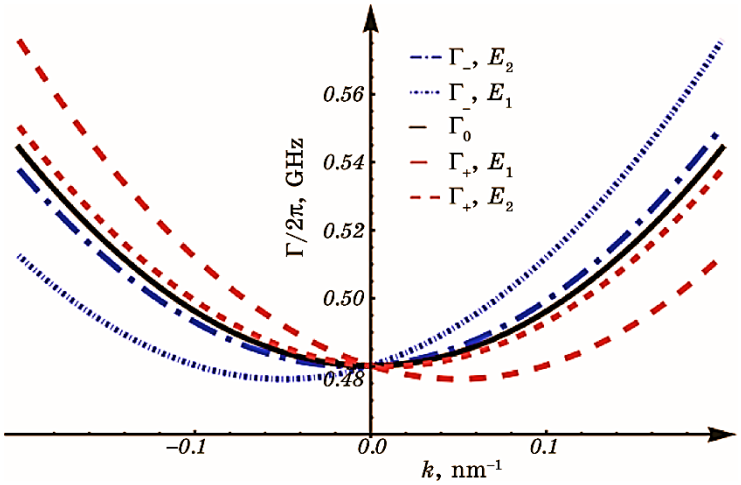

Fig. 3. The electric-field effect on the SWs' damping, Eq. (7): $E_1 = 50$ V/μm, $E_2 = 10$ V/μm. The black line corresponds to $\mathbf{E} = \mathbf{0}$. The damping parameters are $\alpha = 0.01$, $\alpha_c = 0.009$.

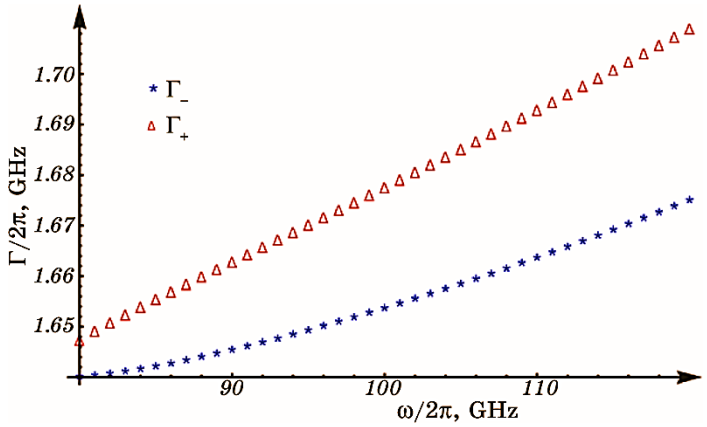

Fig. 4. Influence of the electric field, $E = 50$ V/μm, on the $\Gamma_{\pm}(k)$ magnitude at different values of the corresponding frequency $\omega_{\pm}(k)$. Here, we use the following damping parameters: $\alpha = 0.005$, $\alpha_c = 0.001$.

The peak of the function $\Gamma_{\pm}(k)/\omega_{\pm}(k)$ is shifted along the wave vector axis and proportional to the electric field.

The next factor to be paid attention to is the damping coefficients derived from Rayleigh-dissipation functional. Firstly, the existence of the intersublattice damping, α_c, directly allows the existence of the difference between the temporal attenuation of right- and left-handed polarizations' magnons. When $\alpha_c = 0$, $\Gamma_+(k) = \Gamma_-(k)$. So, the AC effect could

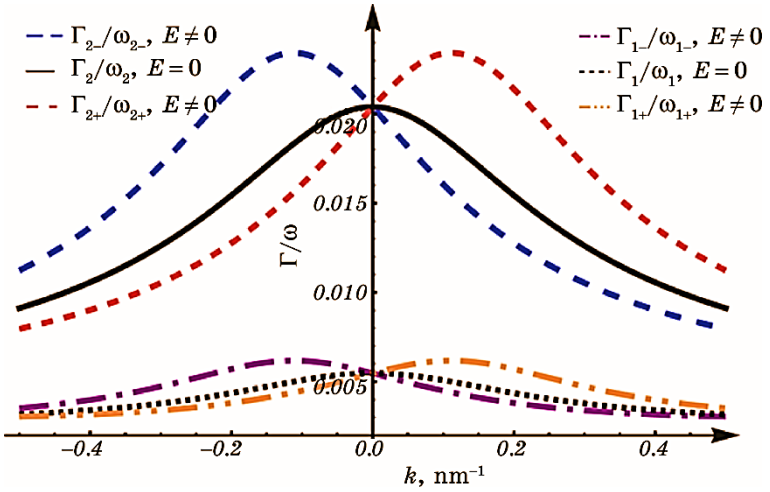

Fig. 5. The electric field $E = 50$ V/μm effect on the dependence $\Gamma_{\pm}(k)/\omega_{\pm}(k)$. The black lines (solid and dotted) correspond to $\mathbf{E} = \mathbf{0}$. Here, we use the next damping parameters: $\alpha = 0.005$, $\alpha_c = 0.004$ ($\Gamma_{1\pm}(k)/\omega_{1\pm}(k)$, dash-dotted lines); $\alpha = 0.005$, $\alpha_c = 0.001$ ($\Gamma_{2\pm}(k)/\omega_{2\pm}(k)$, short and long dashed lines).

help to detect intersublattice damping parameters experimentally.

In insulators, damping parameters could be small 10^{-3}–10^{-4} [21, 22], but the ratio between them can significantly change the dissipation. The coefficient α corresponds to the damping of magnetization dynamics, while α_c has antidamping behaviour. It was shown that these coefficients could be different by several orders of magnitude, at least in Mn-based antiferromagnets [23]. Authors [23] found that the damping coefficient derived from magnon pumping is greater than the Gilbert damping component. It means that a small difference should be between α and α_c, as $\alpha = \alpha_G + \alpha_{sp}$, $\alpha_c \approx \alpha_{sp}$. Thus, the authors [16, 23] point out the importance of taking into account the intersublattice damping.

To the best of our knowledge, there is a lack of similar research for AFM insulators, but we assume that there could be a noticeable difference between α_c and α.

The magnon lifetime is among the important parameters for practical applications. One could find it from the ratio $\tau(k, E) = 1/\Gamma(k, E)$. Figure 6 shows the magnon lifetime of right-handed $\tau_+(k, E)$ and left-handed $\tau_-(k, E)$ modes depending on the electric field. In the absence of an electric field $\tau_+ = \tau_-$, the higher the electric field, the bigger the difference between the magnon lifetimes of different modes. The lifetime difference between the right- and left-handed magnons, depending on the **E** field at different intersublattice parameters, is demonstrated in Fig. 7. The higher the α_c value, the greater the difference between the lifetimes of the right-handed and left-handed SWs.

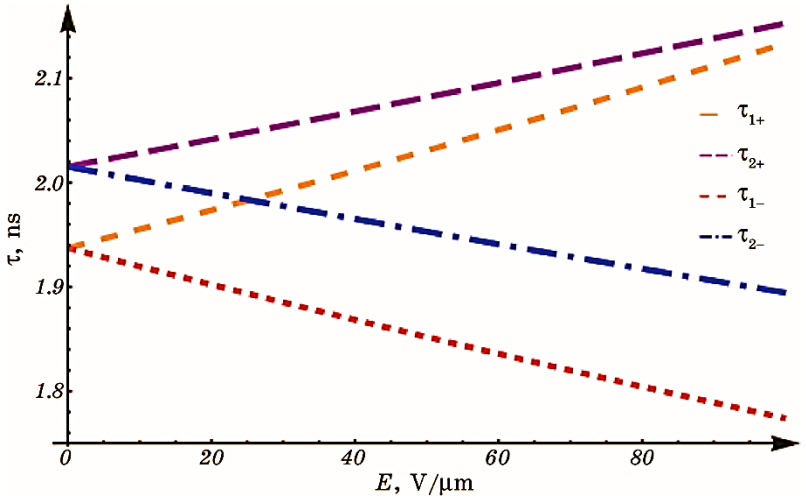

Fig. 6. The magnon lifetime of right-handed (τ_+) and left-handed (τ_-) modes depending on the electric field. $\tau_{1\pm}$ corresponds $k = 0.15$ nm^{-1}, $\tau_{2\pm}$ corresponds $k = 0.1$ nm^{-1}; $E = 50$ V/μm, the damping parameters are: $\alpha = 0.01$, $\alpha_c = 0.009$.

4. DISCUSSION

Condensed matter physics is undergoing a revolution by introducing concepts borrowed from topology to characterize the state and properties of a system. With the introduction of topology, the description of complex systems moves to characterizing their global quantities, which are measured non-locally and endow the system with global stability to disturbances. In magnetism, one vibrant example is the Berry phase—the additional phase that the system's wave function acquires, depending on the trajectory, which it passes [24]. The Aharonov–Casher effect, described in this article, is another special case of the topology phase. The main advantage of such topological effects is their independence from local perturbations, which makes them a very valuable parameter for quantum technologies, spintronics, and magnonics. We could expect that the AC effect will help to create topological magnons [12].

As previously demonstrated in Ref. [7], applying an electric field to an antiferromagnetic insulator, one could split the spin wave spectrum into two independent branches, which we have additionally demonstrated in the example of the system under consideration [13]. The spin waves with right-handed and left-handed polarization could propagate and attenuate separately. The splitting of the spin wave spectrum is achievable by applying a magnetic field, for example, with spin–orbit torque [25]. Nevertheless, an electric field could be a more efficient tool for controlling magnetism without requiring large magnetic

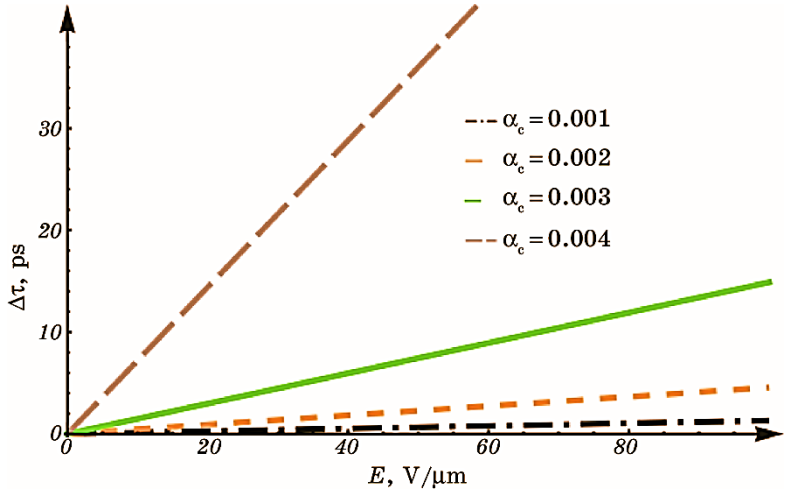

Fig. 7. The difference between the lifetimes of the right-handed and left-handed spin waves depending on the applied electric field at different damping coefficients α_c. Here, $\alpha = 0.005$, $k = 0.05$ nm^{-1}.

fields, which are energetically inefficient and challenging to integrate into nanoscale devices. Moreover, it is applicable for insulating magnetic materials.

There are several examples of practical applications of the AC effect in the SW field-effect transistor [7] or SW interferometric devices [8]. However, these works did not explore the impact of the AC-phase damping on magnon dynamics. Our results show that it could play a significant role in the dynamics of right-handed and left-handed polarized SWs. Considering topological effects like AC-induced without damping could lead to incomplete models that fail to capture real-world behaviour. Damping influences the lifetime and coherence of SWs, which could affect the efficiency of magnonic devices. For instance, the presence of damping can modify the nonreciprocal spin-wave propagation induced by the AC effect, altering its practical applications. Incorporating dissipation into theoretical and experimental studies is essential for accurately predicting device performance.

Integration of the topological effects in magnetism by electric-field control opens exciting prospects for energy-efficient, scalable technologies in spintronics and magnonics. The synergy between topological physics and electric-field-controlled SWs' characteristics is expected to revolutionize next-generation technologies, enabling faster, more energy-efficient, and highly integrative devices.

In conclusion, our work shows how the electric field affects the temporal attenuation of SWs in the insulating AFM. Damping of spin waves with right and left-handed polarizations could be manipulated

independently by the Aharonov–Casher effect. The higher the applied electric field, the more visible this difference. The Aharonov–Casher effect modifies spin-wave dynamics and allows the electric field to control propagation, magnon lifetime, attenuation, and energy of magnons. The difference between the dynamical features of right- and left-handed polarizations of SWs is mainly determined by the applied electric field and the spin–orbit coupling in the material. In contrast to ferromagnets, in antiferromagnets, electric fields allow the use of polarization as an additional degree of freedom, offering new opportunities for designing magnonic devices and topological spin wave logic elements.

This work was partially supported by the National Academy of Sciences of Ukraine through the research program No. 0125U000295 (Innovative materials for quantum sensing).

REFERENCES

1. V. V. Kruglyak, S. O. Demokritov, and D. Grundler, *J. Phys. D: Appl. Phys.*, **43**: 260301 (2010); https://doi.org/10.1088/0022-3727/43/26/260301
2. A. N. Mahmoud, F. Ciubotaru, F. Vanderveken, A. V. Chumak, S. Hamdioui, C. Adelmann, and S. D. Cotofana, *J. Appl. Phys.*, **128**: 161101 (2020); https://doi.org/10.1063/5.0019328
3. Y. Aharonov and A. Casher, *Phys. Rev. Lett.*, **53**: 319 (1984); https://doi.org/10.1103/PhysRevLett.53.319
4. V. N. Krivoruchko, *Low Temp. Phys.*, **46**: 820 (2020); https://doi.org/10.1063/10.0001548
5. Z. Cao, X. Yu, and R. Han, *Phys. Rev. B*, **56**: 5077 (1997); https://doi.org/10.1103/PhysRevB.56.5077
6. T. Liu and G. Vignale, *Phys. Rev. Lett.*, **106**: 247203 (2011); https://doi.org/10.1103/PhysRevLett.106.247203
7. R. Cheng, M. Daniels, J. G. Zhu, and D. Xiao, *Sci. Rep.*, **6**: 24223 (2016); https://doi.org/10.1038/srep24223
8. X. Zhang, T. Liu, M. E. Flatté, and H. X. Tang, *Phys. Rev. Lett.*, **113**: 037202 (2014); https://doi.org/10.1103/PhysRevLett.113.037202
9. R. O. Serha, V. I. Vasyuchka, A. A. Serga, and B. Hillebrands, *Phys. Rev. B*, **108**: L220404 (2023); https://doi.org/10.1103/PhysRevB.108.L220404
10. I. Dzyaloshinskii, *J. Phys. Chem. Solids*, **4**: 241 (1958); https://doi.org/10.1016/0022-3697(58)90076-3
11. T. Moriya, *Phys. Rev. Lett.*, **4**: 228 (1960); https://doi.org/10.1103/PhysRevLett.4.228
12. P. A. McClarty, *Annual Rev. Condens. Matter Phys.*, **13**: 171 (2022); https://doi.org/10.1146/annurev-conmatphys-031620-104715
13. O. Boliasova and V. Krivoruchko, *Phys. Rev. B*, **111**: 174440 (2025); https://doi.org/10.1103/PhysRevB.111.174440
14. R. Cheng, J. Xiao, Q. Niu, and A. Brataas, *Phys. Rev. Lett.*, **113**: 057601 (2014); https://doi.org/10.1103/PhysRevLett.113.057601
15. A. Kamra, R. E. Tronsoco, W. Belzig, and A. Brataas, *Phys. Rev. B*, **98**: 184402 (2018); https://doi.org/10.1103/PhysRevB.98.184402

16. H. Y. Yuan, Q. Liu, K. Xia, Z. Yuan, and X. R. Wang, *Europhys. Lett.*, **126**: 67006 (2019); https://doi.org/10.1209/0295-5075/126/67006
17. A. Kamra and W. Belzig, *Phys. Rev. Lett.*, **119**: 197201 (2017); https://doi.org/10.1103/PhysRevLett.119.197201
18. M. Dehmollaian and C. Caloz, *IEEE Trans. Antennas Propagation*, **69**, Iss. 10: 6531 (2021); https://doi.org/10.1109/TAP.2021.3061262
19. H. V. Gomonay and V. M. Loktev, *Phys. Rev. B*, **81**: 144427 (2010); https://doi.org/10.1103/PhysRevB.81.144427
20. L. Ryzsa, J. Hagemeister, E. Y. Vedmedenko, and R. Wiesendanger, *Phys. Rev. B*, **98**: 100404 (2018); https://doi.org/10.1103/PhysRevB.98.100404
21. P. Trempler, R. Dreyer, P. Geyer, C. Hauser, G. Woltersdorf, and G. Schmidt, *Appl. Phys. Lett.*, **117**: 232401 (2020); https://doi.org/10.1063/5.0026120
22. C. Dubs, O. Surzhenko, R. Linke, A. Danilewsky, U. Brückner, and J. Dellith, *J. Phys. D: Appl. Phys.*, **50**: 204005 (2017); https://doi.org/10.1088/1361-6463/aa6b1c
23. Q. Liu, H. Y. Yuan, K. Xia, and Z. Yuan, *Phys. Rev. Mater.*, **1**: 061401(R) (2017); https://doi.org/10.1103/PhysRevMaterials.1.061401
24. M. V. Berry, *Proc. Royal Society London A*, **392**: 45 (1984); https://doi.org/10.1098/rspa.1984.0023
25. Z. Yan, Z. Li, X. Wang, Z. Luo, Q. Xia, Y. Nie, and G. Guo, *Phys. Rev. B*, **108**: 134432 (2023); https://doi.org/10.1103/PhysRevB.108.134432